

Adsorption Equilibria of Glucose, Fructose, Sucrose, and Fructooligosaccharides on Cation Exchange Resins

Michal Gramblička and Milan Polakovič*

Department of Chemical and Biochemical Engineering, Institute of Chemical and Environmental Engineering, Faculty of Chemical and Food Technology, Slovak University of Technology, Radlinského 9, 812 37 Bratislava, Slovak Republic

The adsorption equilibria relevant to the production of fructooligosaccharides were measured on Dowex Monosphere 99CA/320, Amberlite CR1320Ca, Lewatit S 2568, and Diaion UBK 530. The single-component isotherms of glucose, fructose, and sucrose and multicomponent isotherms of fructooligosaccharides (kestose, nystose, and fructofuranosylnystose) were obtained at a temperature of 60 °C and saccharide concentrations up to about 450 g·L⁻¹. All but sucrose equilibrium data were described with a linear isotherm. The adsorption data of sucrose were successfully fitted using a concave isotherm. The capacities and selectivities of the adsorbents were compared. They showed that their separation effect was based on the size exclusion mechanism accompanied by complexation, which depended significantly on the resin's ionic form.

Introduction

Fructooligosaccharides (FOS) are a group of oligomers containing one glucose unit and 2 to 10 fructose units attached by a β -(2-1) bond.¹ The most common are the three smallest oligomers: kestose, nystose, and fructofuranosylnystose. FOS successfully entered the international market for functional food as food and feed ingredients after their FDA approval in 2000.^{2,3} They are produced industrially either by chemical hydrolysis of inulin from chicory or Jerusalem artichoke or by enzymatic transfructosylation of concentrated sucrose solutions.^{4,5} In the latter case, one glucose molecule is released per transferred fructose molecule. The reactor outlet product contains, besides FOS, a large amount of glucose, unreacted sucrose, and a small portion of fructose, which is produced by the hydrolytic side reaction. These mono- and disaccharides have to be separated from FOS to maintain their functional properties.

Simulated moving bed chromatography (SMB) has been established as the most effective process for the separation and purification of sugar mixtures^{6,7} because their adsorption capacities and selectivities are rather low and the moving bed enhancement is necessary for effective fractionation. SMB is very frequently employed for mono-/disaccharide separations,^{8,9} and the applications for mono-/di-/oligosaccharide separations have also been reported.^{10,11}

At a small scale, FOS have been successfully separated using ion exchangers in either anionic form¹² or, more frequently, in cationic form.¹³ Although ion exchangers are used for the separation, no ion exchange takes place in case of sugars due to their electroneutrality in a wide range of pH. The separation mechanism is based on size exclusion and on complexation of saccharides with functional ions of ion exchangers.^{14,15}

The design of an industrial-scale separation process, including the selection of suitable adsorbent materials, necessitates the knowledge of adsorption equilibria of individual compounds

contained in the feed stream. An extensive work aimed at the separation of mono- and disaccharides has recently been presented by Vente and co-workers.¹⁵⁻¹⁷ They successfully applied both the static method¹⁵ and frontal column experiments.¹⁶ The adsorption equilibria of FOS were investigated only on laboratory grade ion-exchanger beads.¹⁸

The principle objective of this work was the measurement of adsorption isotherms of saccharides of interest on four resins whose potential for the separation was investigated. A static method was employed for measurement of single-component isotherms of glucose, fructose, and sucrose and multicomponent adsorption isotherms of FOS from a commercial mixture.

Experimental Section

Materials. The adsorbents used were Dowex Monosphere 99CA/320 (Dow Chemicals, Midland, MI), Amberlite CR1320Ca (Roehm and Haas, Philadelphia, PA), Lewatit S 2568 (Bayer, Leverkusen, Germany), and Diaion UBK 530 (Mitsubishi Chemical Corporation, Tokyo, Japan). All these resins are in bead form and have a similar polymer nature, which is poly(styrene-*co*-divinylbenzene) matrix, functionalized with $-(SO_3^-)_xMe^{x+}$ groups. The properties of the resins are given in Table 1.

Single-component isotherms were measured using analytical grade chemicals: glucose, fructose, and sucrose (purity ≥ 99 %, Sigma, St. Louis, MO). The source of fructooligosaccharides was a commercial mixture Actilight 950P (Beghin Meiji, Neuilly Sur Seine, France). The composition of this solid mixture determined by HPLC¹³ was as follows: 0.29 % fructose (F), 0.22 % glucose (G), 4.36 % sucrose (GF), 36.48 % kestose (GF₂), 44.54 % nystose (GF₃), 12.21 % fructofuranosylnystose (GF₄), 1.66 % GF₅, and 0.24 % GF₆ (all on mass basis). The saccharide solutions were prepared using double distilled water.

Methods. The adsorption isotherms have been determined using a static method. Each resin was washed several times with distilled water. The extraparticle liquid was removed by suction on a glass frit. Precisely weighed amounts of wet adsorbents

* Corresponding author. E-mail: milan.polakovic@stuba.sk. Phone: +421-2-59325254. Fax: +421-2-52496920.

Table 1. Characteristics of Adsorbents

characteristics	Diaion UBK 530	Dowex Monosphere 99CA/320	Lewatit S 2568	Amberlite CR1320Ca
functional group	$-(\text{SO}_3^-)\text{Na}^+$	$-(\text{SO}_3^-)_2\text{Ca}^{2+}$	$-(\text{SO}_3^-)\text{Na}^+$	$-(\text{SO}_3^-)_2\text{Ca}^{2+}$
mean bead diameter (μm)	220	320	680	320
mass fraction of water ^a (%)	55.2	46.8	52.0	48.1
ion-exchange capacity ($\text{equiv}\cdot\text{L}^{-1}$)	> 1.6	> 1.5	> 1.7	1.63

^a In a wet state, as described in Methods.

Table 2. Single-Component Adsorption Equilibrium Data of Fructose

Diaion UBK 530		Dowex Monosphere 99CA/320		Lewatit S 2568		Amberlite CR1320Ca	
$c/\text{g}\cdot\text{L}^{-1}$	$q/\text{g}\cdot\text{kg}^{-1}$	$c/\text{g}\cdot\text{L}^{-1}$	$q/\text{g}\cdot\text{kg}^{-1}$	$c/\text{g}\cdot\text{L}^{-1}$	$q/\text{g}\cdot\text{kg}^{-1}$	$c/\text{g}\cdot\text{L}^{-1}$	$q/\text{g}\cdot\text{kg}^{-1}$
23.6	16.3	23.7	11.1	23.6	14.3	23.3	14.8
71.1	57.5	47.0	29.0	47.0	33.1	70.0	54.1
94.5	76.8	70.6	46.2	70.8	52.0	93.5	74.5
120.1	102.7	95.0	64.4	95.5	69.7	118.6	91.3
145.1	117.5	118.9	83.5	119.1	92.4	144.0	111.4
169.1	145.3	145.6	98.7	145.1	109.4	198.4	131.2
249.9	204.9	170.5	119.5	171.4	134.6	223.3	160.1
277.8	233.9	196.1	135.5	198.2	150.0	249.7	179.2
307.1	248.4	225.6	159.7	223.2	174.8	304.9	234.8
336.7	266.2	251.1	184.0	252.5	202.1	334.3	258.2
365.6	292.5	281.0	199.5	277.5	225.7	394.8	290.4
398.0	326.1	310.3	209.7	309.6	234.9	422.4	339.3
432.1	332.5	339.9	227.1	337.5	266.2		
		367.5	258.6	365.6	304.2		
		401.2	267.0	396.1	316.5		
		433.7	289.7	429.1	336.8		
Standard Deviation Value of $q/\text{g}\cdot\text{kg}^{-1}$							
linear model		linear model		linear model		linear model	
6.7		5.7		6.1		9.8	

Table 3. Single-Component Adsorption Equilibrium Data of Glucose

Diaion UBK 530		Dowex Monosphere 99CA/320		Lewatit S 2568		Amberlite CR1320Ca	
$c/\text{g}\cdot\text{L}^{-1}$	$q/\text{g}\cdot\text{kg}^{-1}$	$c/\text{g}\cdot\text{L}^{-1}$	$q/\text{g}\cdot\text{kg}^{-1}$	$c/\text{g}\cdot\text{L}^{-1}$	$q/\text{g}\cdot\text{kg}^{-1}$	$c/\text{g}\cdot\text{L}^{-1}$	$q/\text{g}\cdot\text{kg}^{-1}$
21.7	26.0	21.2	11.0	20.3	19.6	20.8	12.9
45.3	41.9	42.6	22.2	41.3	35.8	42.1	26.0
68.2	60.6	64.6	33.6	63.2	50.8	64.8	33.6
93.1	76.4	87.7	37.9	85.6	63.4	87.7	41.6
119.6	83.2	110.7	45.9	108.2	75.7	110.9	51.9
143.8	103.6	134.4	56.0	131.7	92.0	134.4	59.5
167.3	130.2	157.7	72.9	154.9	108.0	157.8	77.3
229.9	161.7	182.9	75.4	178.3	124.0	182.2	82.7
255.0	189.7	236.1	89.1	206.9	145.9	208.7	101.7
334.5	260.6	264.0	87.7	229.3	176.1	234.4	118.2
364.6	257.3	290.6	105.2	257.3	187.9	259.8	134.2
388.8	296.7	315.7	138.6	284.2	207.4	315.3	161.7
		340.2	164.1	311.2	227.7	339.4	184.5
		372.0	158.1	333.4	258.3	368.4	197.8
		399.2	172.7	365.9	260.1	398.7	214.4
				395.6	282.6		
Standard Deviation Value of $q/\text{g}\cdot\text{kg}^{-1}$							
linear model		linear model		linear model		linear model	
8.9		10.5		6.2		6.4	

were transferred into test tubes with a total volume of 10 mL. A specific volume of saccharide solution was added to each test tube. The concentration of sugars in individual solutions ranged from (0 to 450) $\text{g}\cdot\text{L}^{-1}$, with an increment of approximately 25 $\text{g}\cdot\text{L}^{-1}$. The volumetric solid-to-liquid ratio in the suspensions was about 1:2. The test tubes were hermetically sealed and fixed in a horizontal position inside a tempered shaker GFL 1083 (Gesellschaft für Labor Technik, Burgwedel, Germany). The temperature of 60 °C was maintained during the whole sorption process, which was carried out for at least 8 h. Preliminary kinetic experiments proved that this time was

sufficient to reach the equilibrium and to neglect the hydrolysis of sucrose and FOS.¹³

In single-component solutions, the initial and final concentrations of sugars were determined by an Abbe refractometer (Carl Zeiss Jena, Jena, Germany) thermostated at 30 °C. The HPLC system used for the analysis of multicomponent solutions consisted of a column REZEX RSO-Oligosaccharide (Ag^+ form, 200 × 10 mm, Phenomenex, Torrance, CA), a pump LCP 4020 (Ecom, Prague, Czech Republic), on-line degasser model A1050, and a differential refractive index detector type 298.00 operated at 30 °C (both Knauer, Berlin, Germany). The column was

Table 4. Single-Component Adsorption Equilibrium Data of Sucrose

Diaion UBK 530		Dowex Monosphere 99CA/320		Lewatit S 2568		Amberlite CR1320Ca	
$c/\text{g}\cdot\text{L}^{-1}$	$q/\text{g}\cdot\text{kg}^{-1}$	$c/\text{g}\cdot\text{L}^{-1}$	$q/\text{g}\cdot\text{kg}^{-1}$	$c/\text{g}\cdot\text{L}^{-1}$	$q/\text{g}\cdot\text{kg}^{-1}$	$c/\text{g}\cdot\text{L}^{-1}$	$q/\text{g}\cdot\text{kg}^{-1}$
23.5	11.2	23.8	8.0	23.1	15.4	23.8	7.4
47.7	18.8	48.5	11.7	47.2	25.7	48.1	13.0
72.4	28.3	73.5	18.2	71.1	41.8	73.0	21.2
97.3	39.4	99.3	22.0	96.2	54.5	98.2	26.5
122.6	52.8	124.5	34.9	121.2	71.8	123.7	38.4
148.8	60.8	151.1	39.7	146.6	86.2	149.8	45.0
201.9	89.3	176.8	56.7	199.5	116.9	203.3	67.2
228.2	119.0	205.0	58.6	278.4	191.8	231.2	89.2
254.2	152.6	230.8	78.2	309.6	210.0	257.8	107.2
282.0	171.1	287.5	101.1	342.4	230.2	288.1	112.8
311.9	181.9	317.4	109.5	373.9	264.5	346.9	140.1
371.6	213.9	346.7	127.9	440.7	309.6	406.8	180.9
402.5	238.3	376.6	140.1	476.1	316.5	436.3	214.2
434.8	251.7	408.1	153.0				
		441.6	155.4				
Standard Deviation Value of $q/\text{g}\cdot\text{kg}^{-1}$							
linear/concave models		linear/concave models		linear/concave models		linear/concave models	
13.6/9.9		8.1/5.0		9.6/7.7		14.2/4.9	

Table 5. Multicomponent Adsorption Equilibrium Data of Kestose

Diaion UBK 530		Dowex Monosphere 99CA/320		Lewatit S 2568		Amberlite CR1320Ca	
$c/\text{g}\cdot\text{L}^{-1}$	$q/\text{g}\cdot\text{kg}^{-1}$	$c/\text{g}\cdot\text{L}^{-1}$	$q/\text{g}\cdot\text{kg}^{-1}$	$c/\text{g}\cdot\text{L}^{-1}$	$q/\text{g}\cdot\text{kg}^{-1}$	$c/\text{g}\cdot\text{L}^{-1}$	$q/\text{g}\cdot\text{kg}^{-1}$
11.6	4.6	11.6	1.7	11.0	7.6	11.0	8.2
22.8	13.6	23.4	3.4	22.6	13.1	23.8	2.9
35.0	20.3	35.4	7.2	33.8	24.6	36.6	2.1
46.9	31.4	47.6	12.3	46.5	28.2	49.3	3.9
59.8	36.5	60.4	15.0	59.2	34.5	62.0	11.7
73.1	42.3	74.3	11.8	71.8	42.9	75.2	13.8
86.0	55.9	87.8	15.6	85.0	54.1	89.4	15.2
99.7	63.2	101.3	23.2	99.0	59.5	102.2	24.7
112.4	82.4	114.4	33.8	111.2	74.2	118.2	12.4
127.8	89.1	129.5	36.9	125.5	80.6	131.5	27.3
143.7	93.1	144.2	45.3	139.0	99.7	146.3	37.2
159.2	111.5	160.9	41.4	156.2	93.1	161.2	44.6
175.3	120.9	174.6	59.0	170.8	110.3	180.3	34.3
189.8	146.6	192.8	59.7	186.5	135.0	194.9	59.2
207.1	149.5	209.8	60.6	203.5	131.8	213.7	52.5
224.5	176.8	226.7	74.6	218.7	164.3	230.3	63.5
Standard Deviation Value of $q/\text{g}\cdot\text{kg}^{-1}$							
linear model		linear model		linear model		linear model	
7.3		5.5		7.1		7.4	

thermostated at 40 °C using the thermostat Jetstream Plus II (Thermotechnic Products, Langenzersdorf, Austria); 10 μL samples were fed into the system via sampler 234 autoinjector (Gilson, Middleton, WI) at a mobile phase flow rate of 0.3 $\text{mL}\cdot\text{min}^{-1}$.

The equilibrium solid-phase concentration of a saccharide q was determined from the decrease of the saccharide concentration in the liquid phase:

$$q = \frac{V(c_i - c)}{m_a} \quad (1)$$

where V is volume of the bulk liquid phase, c_i and c are the initial and equilibrium concentrations of the solute in the liquid phase. The solid-phase concentration was related to the mass of dry adsorbent, m_a . The water content of wet particles (Table 1) was determined by drying at the temperature of 90 °C until the constant weight was reached.

Results and Discussion

Tables 2 to 4 present the single-component adsorption data of fructose, glucose, and sucrose on four ion-exchange

resins at 60 °C and the liquid-phase concentrations up to about 450 $\text{g}\cdot\text{L}^{-1}$. Such high concentrations are relevant for industrial chromatographic separation. Since pure FOS are available only as very expensive chromatographic standards, their adsorption properties were studied using a solution of their commercial mixture that contained about 5 % of mono- and disaccharides. The multicomponent equilibrium data of FOS are presented in Tables 5 to 7.

Figure 1 presents the adsorption equilibria of glucose on the four ion-exchange resins. This graph illustrates the character of adsorption equilibria for all investigated saccharides but sucrose. A linear dependence between the solid- and liquid-phase concentrations was exhibited, which is very characteristic for saccharide adsorption on ion exchangers.¹⁷ In case of sucrose, the isotherm was slightly curved upward (Figure 2). All experimental data were fitted with the linear isotherm (eq 2) having the single parameter, the distribution coefficient K :

$$q = Kc \quad (2)$$

The equilibrium data for sucrose were moreover fitted with a concave isotherm model (eq 3), which was applied by

Table 6. Multicomponent Adsorption Equilibrium Data of Nystose

Diaion UBK 530		Dowex Monosphere 99CA/320		Lewatit S 2568		Amberlite CR1320Ca	
$c/g \cdot L^{-1}$	$q/g \cdot kg^{-1}$	$c/g \cdot L^{-1}$	$q/g \cdot kg^{-1}$	$c/g \cdot L^{-1}$	$q/g \cdot kg^{-1}$	$c/g \cdot L^{-1}$	$q/g \cdot kg^{-1}$
14.1	3.7	14.1	1.4	13.5	8.2	13.4	9.5
27.9	13.1	28.6	2.7	27.7	13.6	29.2	2.7
42.9	17.9	43.3	5.8	41.4	25.7	44.8	1.9
57.5	29.2	58.3	10.5	57.0	27.6	60.5	4.0
73.4	32.3	74.2	13.9	72.6	35.0	76.1	8.6
89.7	38.6	91.3	9.6	88.2	43.3	92.4	11.9
105.8	49.9	108.0	13.5	104.5	54.6	110.0	9.5
122.8	58.9	124.7	19.7	121.9	68.3	125.9	25.5
138.6	73.9	141.1	28.6	137.0	74.8	145.8	15.6
157.8	79.7	159.8	30.0	154.9	87.6	162.3	32.3
177.7	81.1	178.2	37.9	171.8	110.5	180.8	35.6
197.0	96.3	199.1	34.1	193.3	101.0	199.6	48.8
217.3	107.0	216.4	52.3	211.6	118.1	223.6	37.9
235.6	134.9	239.3	48.1	231.3	140.8	242.0	56.1
257.4	139.1	260.7	51.5	252.8	150.1	265.7	45.5
279.3	160.4	282.2	61.7	272.0	179.0	286.7	58.0
Standard Deviation Value of $q/g \cdot kg^{-1}$							
linear model		linear model		linear model		linear model	
7.3		4.8		8.0		7.2	

Table 7. Multicomponent Adsorption Equilibrium Data of Fructofuranosylnystose

Diaion UBK 530		Dowex Monosphere 99CA/320		Lewatit S 2568		Amberlite CR1320Ca	
$c/g \cdot L^{-1}$	$q/g \cdot kg^{-1}$	$c/g \cdot L^{-1}$	$q/g \cdot kg^{-1}$	$c/g \cdot L^{-1}$	$q/g \cdot kg^{-1}$	$c/g \cdot L^{-1}$	$q/g \cdot kg^{-1}$
3.9	0.6	3.9	0.3	3.7	2.3	3.7	2.0
7.6	2.9	7.8	0.3	7.5	3.5	7.9	0.0
11.6	3.6	11.7	1.0	11.2	6.9	12.1	0.0
15.5	6.5	15.7	2.1	15.4	7.9	16.3	0.0
19.7	6.8	19.9	2.7	19.5	9.1	20.4	1.4
24.0	7.7	24.4	1.4	23.6	11.9	24.7	2.4
28.2	10.8	28.7	2.0	27.8	14.8	29.3	1.9
32.6	12.1	33.0	3.3	32.3	16.5	33.3	5.4
36.6	17.1	37.2	6.5	36.2	19.8	38.4	0.8
41.4	17.2	41.9	6.0	40.7	21.1	42.6	5.1
46.4	16.8	46.5	7.0	44.9	25.6	47.2	7.9
51.2	19.9	51.7	6.7	50.3	25.4	51.8	10.0
56.2	23.9	56.0	11.7	54.8	29.5	57.7	5.7
60.6	30.5	61.5	10.7	59.6	34.9	62.2	11.0
65.8	30.2	66.6	10.6	64.7	34.8	67.8	9.6
71.1	33.9	71.7	13.9	69.3	44.9	72.8	13.4
Standard Deviation Value of $q/g \cdot kg^{-1}$							
linear model		linear model		linear model		linear model	
2.1		1.6		2.1		2.2	

Table 8. Distribution Coefficients: Parameters of Linear Isotherm^a

solute	$K/L \cdot kg^{-1}$			
	Diaion UBK 530	Dowex Monosphere 99CA/320	Lewatit S 2568	Amberlite CR1320Ca
fructose	0.805 ± 0.007	0.685 ± 0.006	0.792 ± 0.006	0.758 ± 0.011
glucose	0.746 ± 0.012	0.420 ± 0.012	0.729 ± 0.007	0.519 ± 0.007
sucrose	0.565 ± 0.015	0.350 ± 0.008	0.675 ± 0.010	0.421 ± 0.016
kestose	0.717 ± 0.014	0.294 ± 0.011	0.674 ± 0.014	0.240 ± 0.014
nystose	0.523 ± 0.011	0.199 ± 0.007	0.589 ± 0.013	0.188 ± 0.011
fructofuranosylnystose	0.436 ± 0.013	0.161 ± 0.009	0.560 ± 0.013	0.143 ± 0.013

^a The value after the ± sign gives the standard deviation.**Table 9. Parameters of Concave Isotherm for Sucrose^a**

parameter	Diaion UBK 530	Dowex Monosphere 99CA/320	Lewatit S 2568	Amberlite CR1320Ca
$B/L^2 \cdot kg^{-2}$	0.39 ± 0.12	0.26 ± 0.06	0.20 ± 0.08	0.54 ± 0.06
$C/L \cdot kg^{-1}$	0.43 ± 0.04	0.26 ± 0.02	0.60 ± 0.03	0.24 ± 0.02

^a The value after the ± sign gives the standard deviation.

other authors for the description of saccharide and polyol adsorption:^{16,19}

$$q = Bc^2 + Cc \quad (3)$$

The quality of the fits of the equilibrium data with the models is illustrated in Figures 1 and 2. The uncertainties are expressed by the standard deviations of solid-phase concentration, which are given in Tables 2 to 7. They were typically in the range of

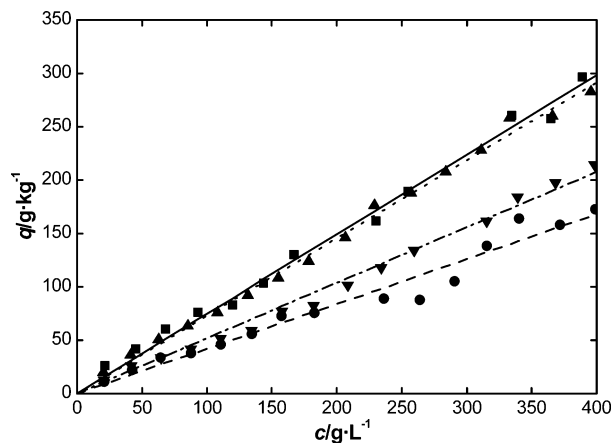


Figure 1. Single-component adsorption equilibria of glucose: ■, —, Diaion UBK 530; ●, ---, Dowex Monosphere 99CA/320; ▲, ···, Lewatit S 2568; ▼, -·-, Amberlite CR1320Ca. The symbols represent experimental data, and the lines are the fits using the linear isotherm model.

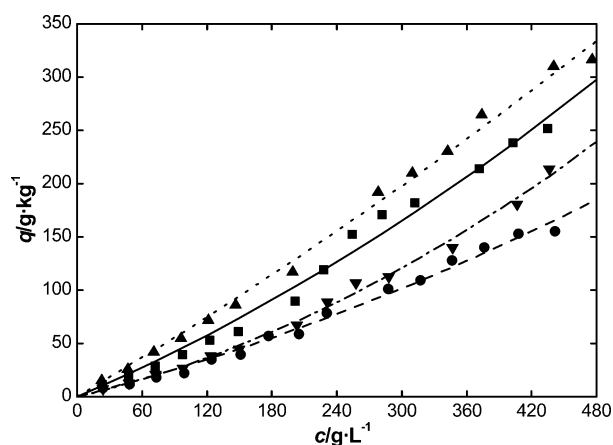


Figure 2. Single-component adsorption equilibria of sucrose: ■, —, Diaion UBK 530; ●, ---, Dowex Monosphere 99CA/320; ▲, ···, Lewatit S 2568; ▼, -·-, Amberlite CR1320Ca. The symbols represent experimental data and the lines are the fits using the concave isotherm model.

(5 to 10) $\text{g}\cdot\text{kg}^{-1}$. The isotherm parameters K , B , and C and their standard deviations are presented in Tables 8 and 9. The lowest uncertainties were obtained at monosaccharides, whose standard deviations of the distribution coefficient were beside one case below 1.5 %. The linear term parameter of the concave isotherm C at sucrose had the uncertainties between 5 % and 10 %, which can be primarily attributed to the cross-correlation with the quadratic term B . The uncertainties of the quadratic term parameter were even higher—from 10 % to 40 %. This is understandable since this term characterizes the deviation from the linear relationship, which was not very strong.

The distribution coefficients in Table 8 and in Figure 3 clearly show that the capacity of the adsorbents in respect to individual saccharides decreased in the order fructose > glucose > sucrose > kestose > nystose > fructofuranosylmystose. It is useful to emphasize that these distribution coefficient values smaller than 1 are, in general, very low for ion-exchange adsorbents. The ion-exchange capacities of adsorbents provided by the producers indicate that if, for example, monosaccharides were bound by a true ion-exchange mechanism, the solid-phase saturation concentration of about $300\text{ g}\cdot\text{L}^{-1}$ would be achieved already at the equilibrium liquid-phase concentration of a few grams per liter.

Since the intraparticle water fractions of these adsorbents were about 50 % (Table 1), the numerical values of the solid-phase concentration per mass of dry adsorbent and per mass of pore

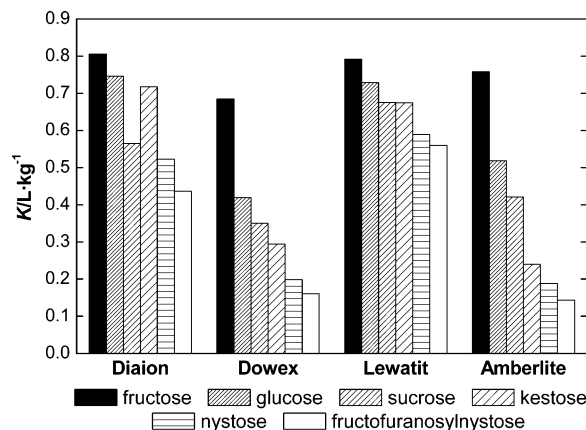


Figure 3. Distribution coefficients obtained using the linear isotherm.

liquid were approximately the same in the equilibrium. The distribution coefficients lower than 1 then implied that the mean intraparticle liquid concentrations were lower than the bulk liquid ones. If the linearity of the isotherms and gradual decrease of distribution coefficients with the molecular weight are furthermore considered, the sieve effect of the resins can be declared as the primary cause of the different partitioning of the investigated saccharides between the solid and liquid phases. This also explains that no effect of the concentration on the distribution coefficients was observed at the multicomponent adsorption from the mixture of FOS. It can then be assumed that the obtained isotherms for individual FOS were not affected by the presence of other species of the mixture. This implies that the ratios of the distribution coefficients could be taken as reasonable approximations of adsorption selectivities.

Another phenomenon contributing to the partitioning of the saccharides was the complexation effect.¹⁵ Its influence is best demonstrated at the differences between the values of the distribution coefficients of glucose and fructose in Table 8 and Figure 3. It is evident that the differences were larger at the Ca-form ion-exchange resins (Dowex Monosphere 99CA/320 and Amberlite CR1320Ca) than at the Na-form ones (Lewatit S 2568 and Diaion UBK 530). A less apparent manifestation of the complexation effect was larger differences among the distribution coefficients of all saccharides at Ca-form ion-exchange resins. The most illustrative difference is between the distribution coefficients of sucrose and kestose on Amberlite CR1320Ca.

The mentioned low capacities of the adsorbents imply a relatively short duration of adsorption–desorption cycles, which makes the implementation of SMB technology effective. However, a good SMB separation necessitates a sufficient selectivity of an adsorbent in respect to key species. A typical composition of saccharides in the feed to the separation section of FOS production is as follows: FOS 55 % (mass), glucose 31 %, sucrose 12 %, and fructose 2 %.²⁰ A typical design of FOS separation requires a yield higher than 95 % when the raffinate should contain at least 95 % of FOS. The key species at the design of FOS chromatographic separation cascade are then sucrose and kestose, but a good selectivity of glucose to kestose is important too. Table 8 shows that the Na-form resins (Lewatit S 2568 and Diaion UBK 530) had the sucrose/kestose selectivity (approximated from the ratio of their distribution coefficients) close to 1, and they would not be effective in this application. The sucrose/kestose selectivities of the Ca-form ion-exchange resins (Dowex Monosphere 99CA/320 and Amberlite

CR1320Ca) were 1.2 and 1.75, respectively. The Amberlite had also a much better glucose/kestose selectivity of 2.2 as compared to the value of 1.4 for the Dowex.

Conclusions

A static method was used to measure equilibrium isotherms of saccharides on several ion-exchange resins at industrial process conditions. The results proved that the size exclusion effect is a key factor at separation of oligosaccharides using PS-DVB ion exchangers. The ionic form also significantly affects the adsorption, due to different extent of complexation of functional ions with particular sugar molecules. Dowex Monosphere 99CA/320 and Amberlite CR1320Ca were clearly more suited for proposed separation in comparison with other two resins due to their higher selectivities in examined ionic form.

Literature Cited

- (1) Yun, J. W. fructooligosaccharides—occurrence, preparation, and application. *Enzyme Microb. Technol.* **1996**, *19*, 107–117.
- (2) Sangeetha, P. T.; Ramesh, M. N.; Prapulla, S. G. Recent trends in the microbial production, analysis and applications of fructooligosaccharides. *Trends Food Sci. Technol.* **2005**, *16*, 442–457.
- (3) Bornet, F. R. J.; Brouns, F.; Tashiro, Y.; Duvillier, V. Nutritional aspects of short-chain fructooligosaccharides: natural occurrence, chemistry, physiology and health implications. *Dig. Liver Dis.* **2002**, *34*, 111–120.
- (4) Cabral J. M. S.; Best D.; Boross L.; Tramper J. *Applied Biocatalysis*; Harwood Academic Publishers: Amsterdam, 1994.
- (5) Sangeetha, P. T.; Ramesh, M. N.; Prapulla, S. G. Maximization of fructooligosaccharide production by two stage continuous process and its scale up. *J. Food Eng.* **2005**, *68*, 57–64.
- (6) Paananen, H. A. Trends in chromatographic separation of molasses. *Zuckerindustrie* **1997**, *122*, 28–33.
- (7) Bubnik, Z.; Pour, Z.; Gruberova, A.; Starhova, H.; Hlinkova, A.; Kadlec, P. Application of continuous chromatographic separation in sugar processing. *J. Food Eng.* **2004**, *61*, 509–513.
- (8) Kishihara, S.; Fujii, S.; Tamaki, H.; Kim, K. B.; Wakiuchi, N.; Yamamoto, T. Continuous separation of sucrose, glucose and fructose using a simulated moving-bed adsorber. *Intl. Sugar J.* **1992**, *94*, 305–208.
- (9) Lee, K. N. Continuous separation of glucose and fructose at high concentration using two-section simulated moving bed process. *Kor. J. Chem. Eng.* **2003**, *20*, 532–537.
- (10) Kim, K. B.; Kishihara, S.; Fujii, S. Simultaneously continuous separation of glucose, maltose, and maltotriose using a simulated moving-bed adsorber. *Biosci. Biotechnol. Biochem.* **1992**, *56*, 801–802.
- (11) Geisser, A.; Heindrich, T.; Boehm, G.; Stahl, B. Separation of lactose from human milk oligosaccharides with simulated moving bed chromatography. *J. Chromatogr. A* **2005**, *1092*, 17–23.
- (12) Shiomi, N.; Onodera, S.; Chatterton, N. J.; Harrison, P. A. Separation of fructooligosaccharide isomers by anion-exchange chromatography. *Agric. Biol. Chem.* **1991**, *55*, 1427–1428.
- (13) Antořová, M.; Polakovič, M.; Bálež, V. Separation of fructooligosaccharides on a cation-exchange HPLC column in silver form with refractometric detection. *Biotechnol. Technol.* **1999**, *13*, 889–892.
- (14) Goulding, R. W. Liquid chromatography of sugars and related polyhydric alcohols on cation exchangers. *J. Chromatogr.* **1975**, *103*, 229–239.
- (15) Vente, J. A.; Bosch, H.; de Haan, A. B.; Bussmann, P. J. T. Comparison of sorption isotherms of mono- and disaccharides relevant to oligosaccharide separations for Na, K, and Ca loaded cation exchange resins. *Chem. Eng. Commun.* **2005**, *192*, 23–33.
- (16) Vente, J. A.; Bosch, H.; de Haan, A. B.; Bussmann, P. J. T. Evaluation of sugar sorption isotherm measurement by frontal analysis under industrial processing conditions. *J. Chromatogr. A* **2005**, *1066*, 71–79.
- (17) Vente J. A. Adsorbent functionality in relation to selectivity and capacity in oligosaccharide separations. Ph.D. Thesis, University of Twente, Netherlands, 2005.
- (18) Takahashi, Y.; Goto, S. Continuous separation of fructooligosaccharides using an annular chromatograph. *Sep. Sci. Technol.* **1994**, *29*, 1311–1318.
- (19) Muralidharan, P. K.; Ching, C. B. Determination of multicomponent adsorption equilibria by liquid chromatography. *Ind. Eng. Chem. Res.* **1997**, *36*, 407–413.
- (20) Madlová, A.; Antořová, M.; Polakovič, M.; Bálež, V. Thermal stability of fructosyltransferase from *Aureobasidium pullulans*. *Chem. Pap.* **2000**, *54*, 339–344.

Received for review April 20, 2006. Accepted December 2, 2006. This study was supported by the Slovak Grant Agency for Science VEGA (Grant 1/3565/06) and the Agency for Support of Research and Development (Grant APVT-20–025704).

JE060169D